A Novel Mechanical-Based Injective Hydrogel for Treatment with Aromatase Inhibitors Caused Joint Inflammation via the NF-κB Pathway

Zipeng Yang, Chang-Peng Xu, Yuhui Chen, Wenqiang Li,* Liping Wang,* and Zi-Guo Yuan*

ACCESS | Metrics & More | Article Recommendations

ABSTRACT: Synovium has widely participated in induced inflammation, suggesting that it is a potential target to reduce aromatase inhibitors (AIs) causing joint inflammation or pain. Exercise and mechanical stimulation are important strategies for precaution and treatment of bone inflammation. In this work, we developed a novel thermo-sensitive hydrogel, which could be injected intra-articularly. The aim of this research was to investigate the role of various mechanical strength hydrogels in reducing synovium inflammation. The effect of different mechanical strength hydrogels on regulating synovium inflammation was used to stimulate human fibroblast-like synoviocytes (FLS) under a cyclic mechanical compression environment *in vitro*. Cytokine and metalloprotease expression in FLS was analyzed by the western blot and q-PCR method, in which FLS were cultured with the different mechanical strength hydrogels. The results showed that a moderate-intensity hydrogel mechanical stimulation might be suitable in reducing AI-induced FLS inflammation via the NK-κB pathway. In addition, we built an AI-treated rat model and injected the different mechanical strength hydrogels. Similarly, the moderate-strength mechanical hydrogel could reduce the inflammatory factor and metalloproteinase expression in synovial tissues and intra-articular synovia.

1. INTRODUCTION

Many clinical data indicate a negative effect of aromatase inhibitors (AIs) on joints and joint pain in breast cancer studies.[1−3] AIs are widely used in postmenopausal hormone receptor−positive breast cancer patients.[4] However, musculoskeletal symptoms, such as morning stiffness, often happen and reduce treatment tolerability. Thus, morning stiffness and joint pain often occurred during AI therapy.[5] Additionally, AIs may regulate the estrogens to arouse inflammation.[6−9] When aromatase is blocked by AIs and then estrogen is reduced, it transforms to pro-inflammatory 16-OH estrogens and further triggers inflammation.[10] The excess inflammation will furthermore stimulate cells to secrete pain mediators.[11] Therefore, joint pain or morning stiffness occurred after AI treatments. However, there are few valid methods to limit joint excess inflammation during the AI treatment phase. Thus,

controlling inflammation may be a key to counter the side effect of AIs toward joint pain.

Among the therapeutic schedules, exercise and mechanical stimulation therapy are important strategies to prevent and treat joint inflammation.[12] Studies have shown that, compared with non-exercising participants, the patients who exercise according to their personal conditions possessed an effective improvement in knee osteoarthritis.[13] Fibroblast-like synoviocytes (FLS), spread among the synovium, served an important role in lubricating, nourishing chondrocytes, and maintaining
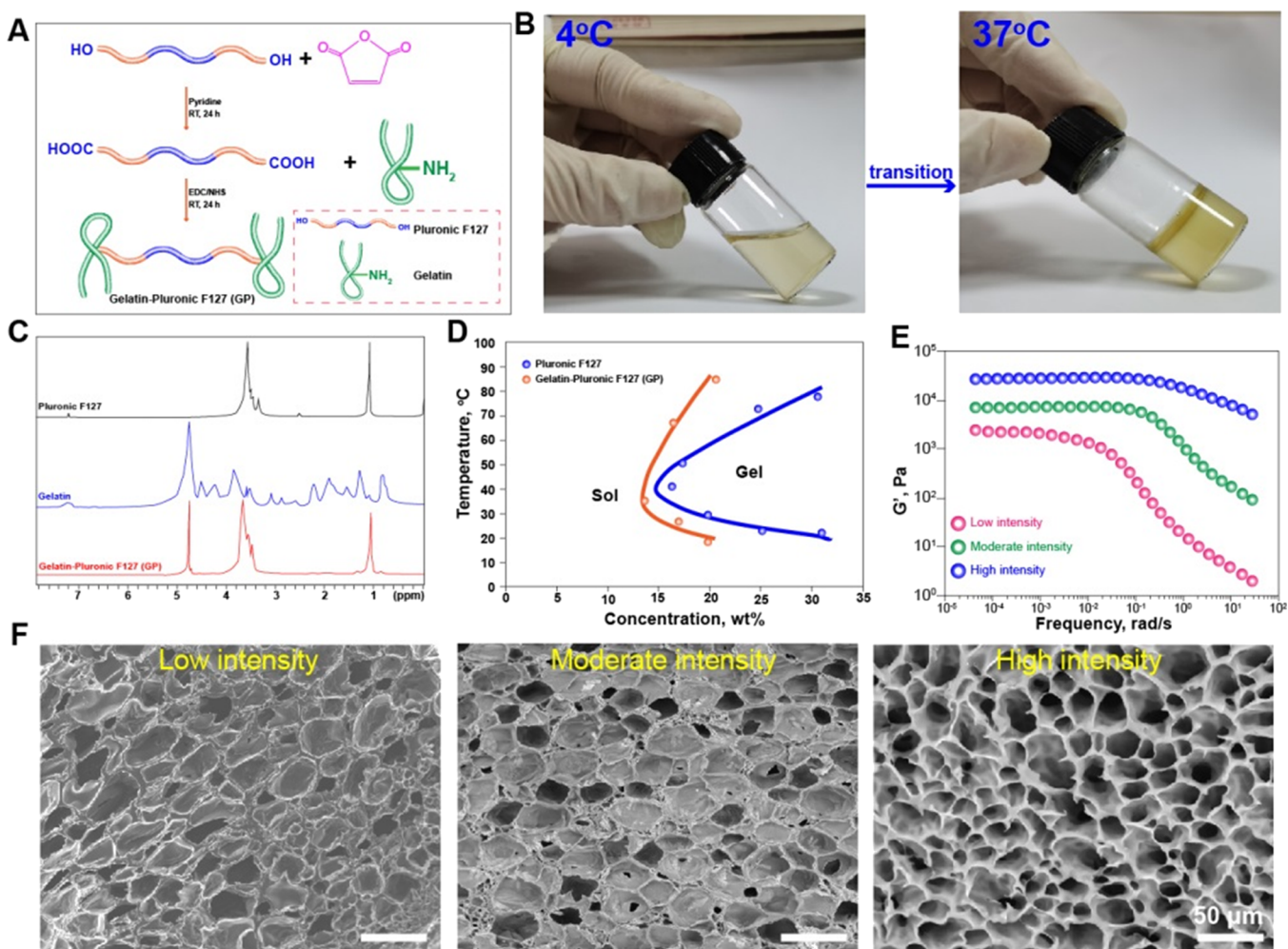
Figure 1. (A) Synthetic circuit diagram of gelatin-grafted Pluronic; (B) images of the hydrogel production process; (C) ^{1}H NMR spectra of Pluronic, gelatin, and GP; (D) phase diagram of Pluronic and GP; (E) oscillatory frequency sweep tests (at a strain of 0.05%) at 37 °C; and (F) SEM images of GP hydrogels of different stiffness values.

cartilage by secreting synovial fluid and inflammation-related factors.[14] The synovium is tightly attached to the inner surface of the articular capsule, which possesses a wider movement space. Similarly, the FLS are constantly exposed to a dynamic mechanical stimulation that came from the body weight and synovial fluid shear forces during exercise.[15] FLS contribute to the initial function of producing pro-inflammatory cytokines, such as interleukin IL-6, IL-1β, and tumor necrosis factor (TNF)-α, and the other small-molecule inflammation factor causing joint injury or pain.[16] However, how to utilize the relationship of mechanical stress and inflammatory mediators to affect the FLS function remains unclear.[17−19] Based on biomechanics, this work first aims to reduce the inflammation level via giving different mechanical stimulations on FLS during the AI treatment phase.

This study aimed to prepare a hydrogel with adjustable mechanical properties and analyzed the morphology and mechanical properties. Furthermore, we evaluated the responses of hydrogel mechanical stimulation on inflammatory for FLS derived from AI-treated rats. The cell proliferation, apoptosis, inflammation-related genes and protein expression have been analyzed. Moreover, we injected the hydrogel intra-articularly and analyzed the expression of inflammation expression of IL-6 and MMP-1 via an immunohistochemical

(IHC) and ELISA method. Therefore, the prepared hydrogels with proper mechanical strength have potential applications as inflammation-regulating systems in AI-treated joint pain therapy.

2. RESULTS AND DISCUSSION

**2.1. Characterization Analysis of the Hydrogel.** We successfully developed an injectable thermal-responsive hydrogel, performing sol−gel phase transition by stimulating the body temperature, which could improve mechanical stability and biocompatibility. Gelatin is a promising material for implantation due to its biodegradability, biocompatibility, non-antigenicity, renewable ability, various active groups for targeting molecules, and high stability during storage. Thus, we choose gelatin as a preferred material to modify Pluronic F127. Figure 1A shows that gelatin was directly coupled with Pluronic F127 to form a gelatin-grafted Pluronic (GP) thermo-sensitive polymer by acylation reaction of amidogen and the carboxyl group, and the GP system completed the sol−gel transition at 37 °C for a 15% w/v concentration (Figure 1B). As shown in Figure 1C, the peaks at 4.8 ppm for anomeric carbon, 1.9−4.0 ppm for alkyl protons, and 3.1 ppm for amino carbon appeared for the gelatin characteristic peak. In addition, the peaks at 3.0−3.5 ppm for $CH_2−CH_2$ and the peak at 1.11
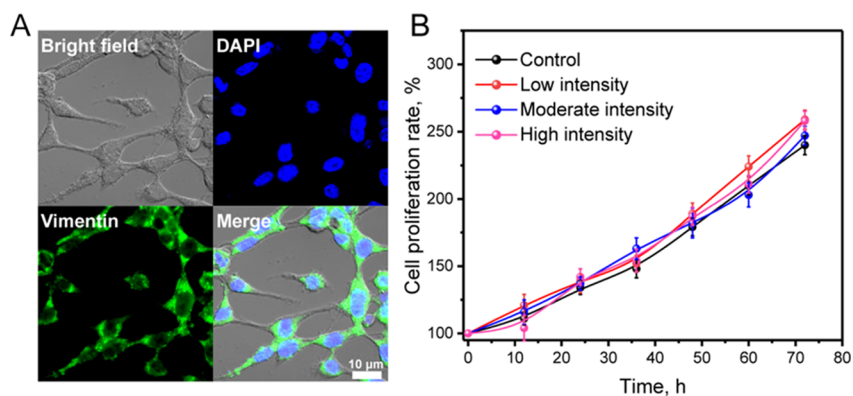
Figure 2. Synovial fibroblasts' cell viability cultured with low-intensity, moderate-intensity, and high-intensity hydrogels at different times. (A) The cells were stained by vimentin immunofluorescence and DAPI. (B) The cell proliferation rate was measured by the MTT method.

ppm for the methyl group appeared for the Pluronic characteristic peak. Similarly, the protons (4.78 ppm), alkyl protons (1.93−4.18 ppm), and two peaks (CH$_2$−CH$_2$, 3.1−3.7 ppm) were observed on the GP hydrogel, which indicated the successful synthesis of gelatin-grafted Pluronic copolymers. It can be seen from the phase diagram of Pluronic and GP that the change of the gel temperature was related to the concentration (Figure 1D). The gel temperature range of GP was wider than that of Pluronic due to the reversible gel properties of gelatin around the body temperature. The mechanical performance (elasticity behavior) of GP hydrogels with different intensities was evaluated by rheological tests, as shown in Figure 1E. Different concentrations of GP hydrogels (5, 10, and 15% (w/v)) exhibited a representative frequency-independent behavior. As expected, the high-intensity sample had the highest G' values because of a higher cross-linking density, which was consistent with the SEM results. As shown in Figure 1F, all three groups of hydrogels presented a three-dimensional porous morphology. Compared with the other two groups, the high-intensity scaffold presented a groove-like structure with a relatively uniform fracture surface due to a high cross-linking point.

2.2. Effects of Different Mechanical Stimulations on Cell Cytotoxicity and Apoptosis.

Primary FLS were obtained from the rat knee synovium, observed by an optical microscope, and identified by staining with vimentin in immunofluorescence.[20] Vimentin is an important skeleton protein that maintains the cellular structure and is involved in mechanical pressure regulation between cells and the surrounding matrix. It is mainly expressed in FLS, white blood cells, and endothelial cells and is closely related to cell growth, apoptosis, signal transduction, adhesion, and migration. It can be seen that the primary FLS isolated from the synovial tissue were in a uniform spindle shape with a striking expression of vimentin, as shown in Figure 2A. The cell proliferation and viability results are presented in Figure 2B, and we found that hydrogels with different mechanical strengths had no negative effect on synovial fibroblasts. In the four groups (control, low strength, moderate strength, and high strength), all the cell numbers increased without significant differences, which demonstrated that the inflammatory gene or protein expression was irrelevant to apoptotic or cytotoxic effects. To further investigate the mechanical stimulation effect on cytotoxicity, we conducted the apoptosis analysis using Annexin V-FITC and PI double staining flow cytometry as shown in Figure 3. There was no obvious
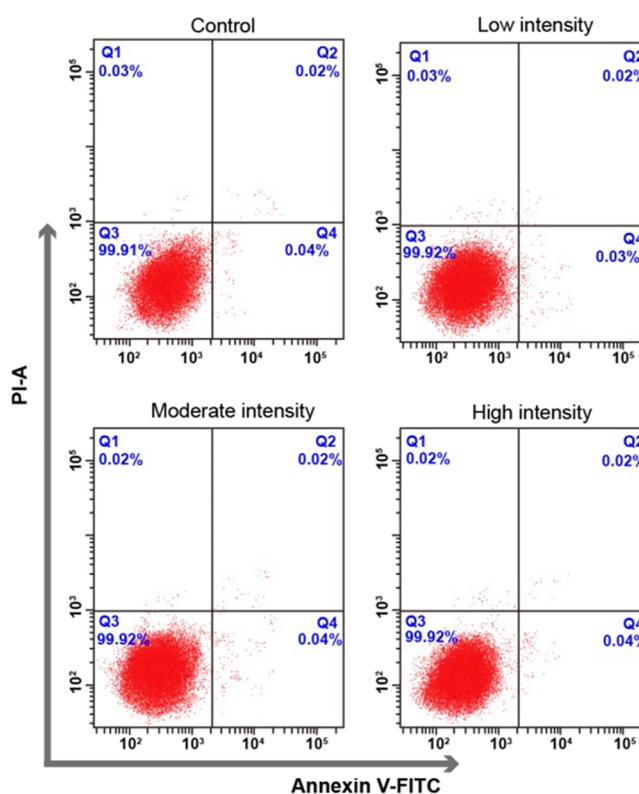

Figure 3. Synovial fibroblasts' cell viability cultured with low-intensity, moderate-intensity, and high-intensity hydrogels at 72 h at cyclic compression pressure. The cells apoptosis was analyzed by flow cytometry.

apoptosis in FLS treated with hydrogels of different mechanical strengths, and the total apoptosis rate was less than 1.0% as well as with the control group. The above results reconfirmed that the effect of mechanical stimulation on FLS would not lead to apoptosis *in vitro*.

2.3. Effects of Hydrogels with Various Strengths on Inflammatory Gene Expression.

The previous literature has shown that a variety of stimulation can activate FLS and induce inflammation and arthralgia, such as cytokines, growth factors, adipokines, and drugs.[21−23] To research the impact of mechanical strength on inflammation-related processes, we chose three hydrogels with different mechanical strengths subjected to cyclic compression pressure simulating sports cycle to study inflammation mRNA expression. When applying
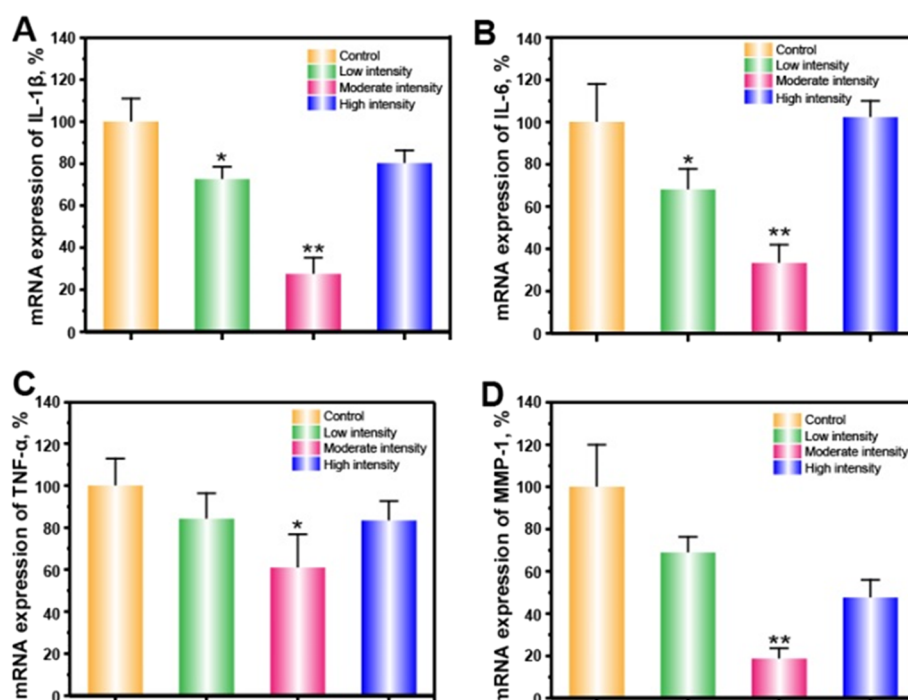
Figure 4. The effect of different mechanical intensities of the hydrogel on inflammatory agent mRNA expression in the FLS was demonstrated. The mRNA expression levels of bone markers IL-1β (A), IL-6 (B), TNF-α (C), and MMP-1 (D) at 24 h were detected by qPCR.
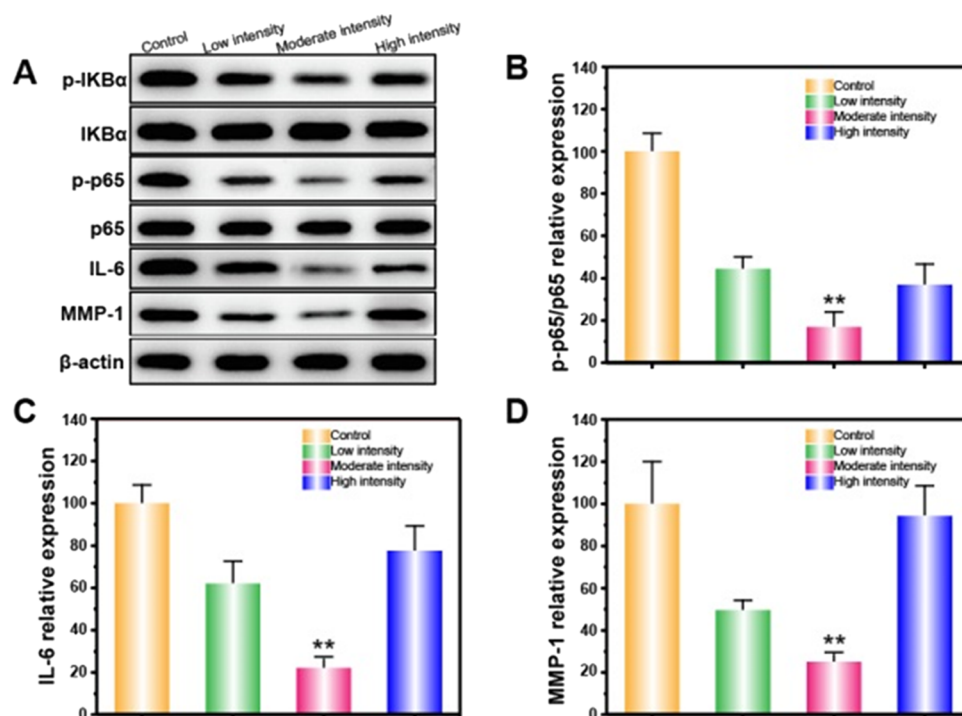
Figure 5. Western blotting showed protein levels of p-IKBα, IKBα, p-p65, p65, IL-6, and MMP-1 at 24 h (A). Statistical analysis of the relative protein expression of p-p65/p65 (B), IL-6 (C), and MMP-1 (D) at 24 h. All data are the average values from several independent experiments ($n = 3$). *$P < 0.05$, **$P < 0.01$ vs the control group.

moderate-strength hydrogels, IL-1β, IL-6, TNF-α, and MMP-1 gene expressions were significantly reduced (Figure 4). The low-strength hydrogel group could affect IL-1β and IL-6 gene expressions slightly ($p < 0.01$). In contrast, high-strength hydrogels enhance inflammatory gene expression significantly, indicating that a high mechanical stimulation led to intensive inflammatory gene generation. This result further supported

the finding that different mechanical strength stimulations influenced inflammatory gene expression in synovial fibroblasts.[24] In addition, moderate-strength hydrogels appeared to prevent the inflammatory gene expression in FLS. The result illustrated that the relationship between the mechanical stimulation and biological effect is not a simple linear relation. The process of regulating synovial cell inflammatory factor
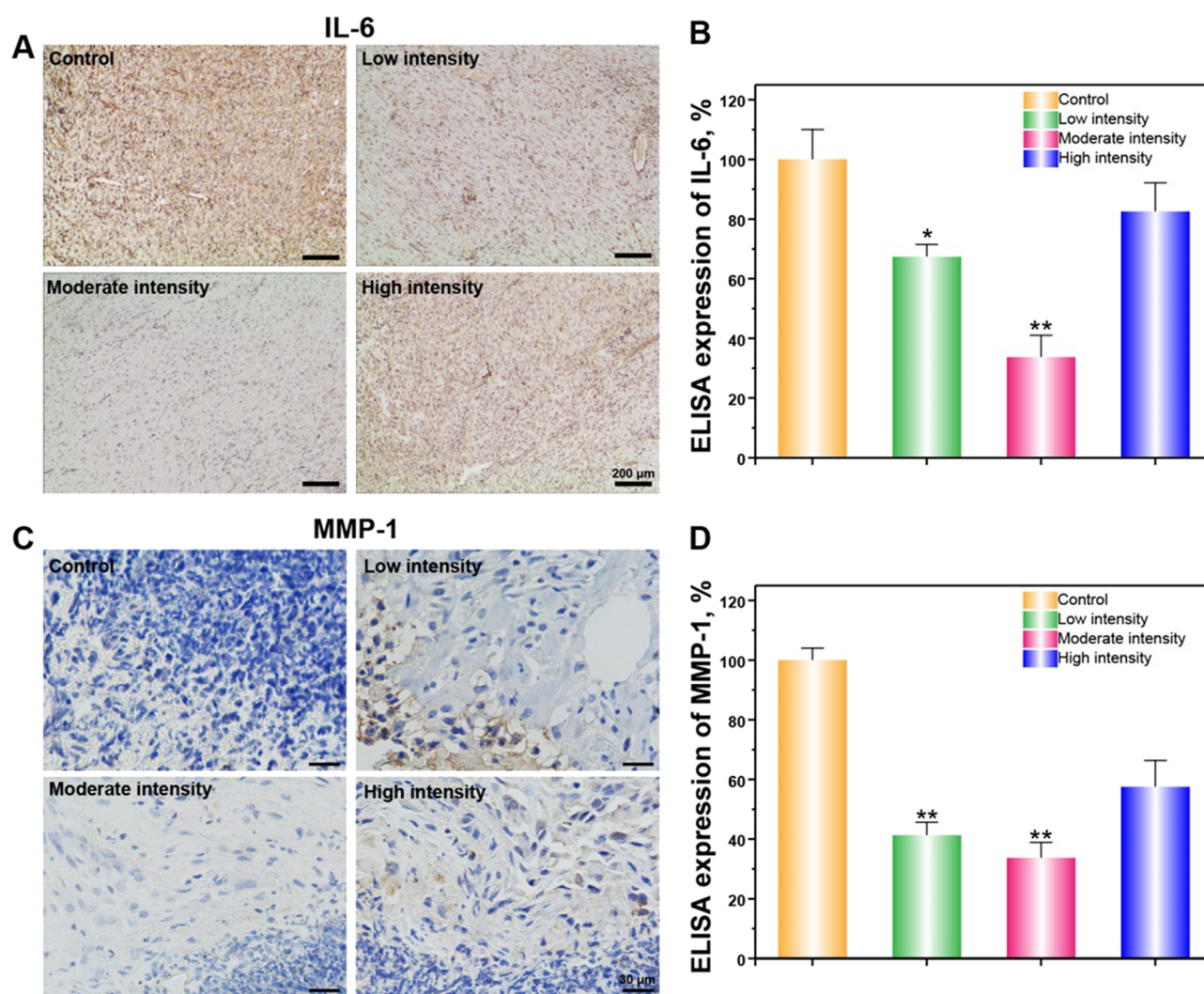
Figure 6. Immunohistochemical image of IL-6 (A) and MMP-1 (C) expressions in synovial tissues after injection of different strength hydrogels at week 2. Quantitative analysis of IL-6 (B) and MMP-1 (D) expressions in intra-articular synovia after injection of different strength hydrogels at week 2. All experiments were conducted in triplicate. *$P < 0.05$, **$P < 0.01$ vs the control group. The scale bars are 200 (A) and 30 μm (C), respectively.

secretion is also complex, which depends on actual experimental data. Neither too high nor too low mechanical strength is sufficient to reduce the secretion of inflammation by synovial cells.

2.4. Effects of Different Mechanical Stimulations on the NF-κB Pathway. Among multiple pathways and mediators influencing the development and persistence of synovial inflammation, NF-κB is reported to play a prominent role.[25] Excessive mechanical stress, pro-inflammatory cytokines, and matrix degradation enzymes could trigger the phosphorylation and IκB degradation by the ubiquitin proteasome. Whereafter, active NF-κB (p65/p50) was released due to the degradation of IκB and transferred to the nucleus for the transcriptional induction of genes (IL-6 and MMP-1).[26] In the inflammation processes, FLS were activated to secrete matrix-degrading proteinase. Thus, the articular cartilage was destroyed by secretion of MMPs and turned chondrocytes to switch to a derivative phenotype, resulting in more pain. We studied the effect of hydrogels with different strengths on inflammatory protein expression. It can be seen that the expression of p-IK$\beta\alpha$/IK$\beta\alpha$ and p-p65/p65 was significantly reduced when FLS were cultured with moderate-strength

hydrogels. Further, the inflammatory factor expressions such as IL-6 and MMP-1 were also decreased, indicating that the NF-κB pathway was inhibited by moderate-strength hydrogels (Figure 5). By contrast, when the FLS were cultured with low- and high-strength hydrogels, the NF-κB pathway was stronger than in the moderate-strength hydrogel group. The results suggest that AI-treated FLS suffered inflammatory insults and impacted the molecular functions of synovial fibroblasts. In particular, the different mechanisms of the hydrogel altered the AI-associated inflammation by regulating the NF-κB pathway. This result was in accordance with the previous studies, suggesting that mechanical stretching enhances the expression of NF-κB-dependent genes in synovial cells.[27]

2.5. Effects of Different Mechanical Stimulations on Inflammatory Factor Expression in Rats. In order to investigate the mechanical stimulation on the inflammatory factor, the different mechanical strength hydrogels were injected intra-articularly for 2 weeks. The aggregation of inflammatory cells and the expression of IL-6 and MMP-1 in the synovial intima and subintima were observed in synovial tissues by an immunohistochemical method. It can be seen from the immunohistochemical image that, in the AI-pre-

Table 1. qRT-PCR Primers for Analysis of Gene Expression

primer	5′ forward 3′	5′ reverse 3′
IL-6	GCCACTCACTTCTTCAGAA	GTACTCATCTGCAGCT
IL-1β	CTGCCTGCGTGTTGAAAGA	TTGGTAATTTGGGGATCTACA
MMP-1	TACCATCCTGCGACTCTTGC	TTCACCCACATCAGGCACTC
GAPDH	CAAAGTTTCATGGATGACC	CCATGGAAGGCTGGG

treated synovial membrane, IL-6 and MMP-1 positive cells were abundant in the synovial inner layer, and the sub-synovial layer was diffused (Figure 6A,C). When intra-articularly was injected into the low- or moderate-strength hydrogel, the expressions of IL-6 and MMP-1 were decreased significantly, indicating that the suitable intensity of mechanical stimulation could reduce inflammation expression. In contrast, the high-intensity mechanical stimulation could not effectively reduce the inflammation expression. To verify the IHC result accuracy, the quantitative analysis was conducted using an ELISA kit. It can be seen that the expressions of IL-6 and MMP-1 were also decreased in the intra-articular synovia treated with a moderate-strength hydrogel. This ELISA quantitative data was in accordance with the IHC image. For the clinical application, in a patient who has severe joint inflammation or pain, the mechanical-based injective hydrogel could be injected intra-articularly. Following the cyclic compression exercise, the FLS received favorable mechanical stimulation to reduce inflammatory factor secretion.

3. CONCLUSIONS

In the process of AI-related joint pain inflammation, fibroblast-like synoviocytes (FLS) play an important role. In the process, the NF-κB pathway was highly activated in FLS and is the main cause associated with joint pain. In our research, a different mechanical strength hydrogel that could be injected intra-articularly have developed. *In vitro*, we obtained FLS from the AI-treated rats and cultured them with different mechanical strength hydrogels under a cycle compression pressure simulating sports. The hydrogel has also shown that it could significantly inhibit the activation of the NF-κB pathway and the release of inflammatory factors. In particular, the medium-strength hydrogel significantly inhibited synovium inflammation of the joint, which was induced by AIs. Therefore, these results demonstrated that a strategy of an injectable hydrogel with an appropriate mechanical strength was a potential inflammatory control method concerning AI-related joint pain.

4. EXPERIMENTAL SECTION

4.1. Materials and Reagents. Pluronic F127, 1,6-diisocyanatohexane, gelatin, 1-ethyl-3-(3-dimethylaminopropyl)carbodiimide (EDC)/N-hydroxysuccinimide (NHS), succinic anhydride, and 4-morpholineethanesulfonic acid (MES) were purchased from Sigma-Aldrich. Biomedical agents were obtained from Thermo Fisher Scientific. All other chemicals were used as received.

4.2. Preparation of the Thermo-sensitive Hydrogel (Gelatin-Pluronic, GP). First, Pluronic was carboxylated with succinic anhydride to prepare carboxylated Pluronic according to a previous method.[28] Then, gelatin-grafted Pluronic (GP) hydrogels with different stiffness values were produced by adjusting the gelatin concentration. In brief, hydrogel scaffolds with different mechanical strengths (low, moderate, and high intensity) were obtained by containing 5, 10, and 15% (w/v) gelatin, respectively. The cross-linking reaction occurred by adding carboxylated Pluronic and gelatin with EDC/NHS as the cross-linking agent at R.T. for 24 h.

An ^{1}H NMR spectrometer (Bruker Biospin GmbH, Germany) was used to characterize the obtained product structure, and phase transition behavior measurement of Pluronic and GP was measured by the vial tilting method with the temperature ranging from 0 to100 °C at various concentrations. The rheological tests were conducted by a rotational rheometer (DHR, TA Instruments, USA) to monitor storage (elastic) modulus G' and loss (viscous) modulus G'' versus temperature with the angular frequency ranging from 0.1 to 100 rad/s under a fixed strain level of 0.005% at 37 °C. Meanwhile, the GP hydrogel morphology with different stiffness values was analyzed by a field emission scanning electron microscope (ULTRA 55, Carl Zeiss, Germany).

4.3. Fibroblast-like Synoviocyte (FLS) Isolation and Culture. Fibroblast-like synoviocytes (FLS) were obtained from the synovial tissue of knee joints of female SD rats (6 weeks old; specific pathogen-free). Before the cells were taken, the female rats were feed with AI drugs for 5 weeks. The synovial tissue was collected, cut into pieces in sterile PBS, and incubated with collagenase D (1 mg/mL, Roche, Switzerland) at 37 °C under vibration for 2 h followed by incubation with trypsin (0.1%, Biological Industries, Israel) at 37 °C for 20 min. FLS were cultured in 25 cm^2 cell culture flasks in DMEM (HyClone, USA) containing 10% fetal bovine serum (Clark, USA) and antibiotics (100 U/mL penicillin and 100 μg/mL streptomycin) in 5% CO$_2$ at 37 °C. The medium was refreshed every 2 days.

4.4. Cell Mechanics Loader Culture System. FLS were seeded into Petri dishes (1 × 10^4 cells/piece) contained by polyvinyl-alcohol-based scaffolds. FLS in scaffolds were transplanted into the computer-controlled bioreactor (Electro-Force3200, BOSE, BioDynamic, USA) and cultured with three kinds of mechanical strength of hydrogels. The FLS were subjected to cyclic compression pressure simulating sports cycle (20 and 40 kPa were applied at 0.5 Hz) up to 24 h. FLS in the control group were cultured with DMEM complete medium conditions.

4.5. FLS Culture Conditions, Proliferation, and Apoptosis. FLS cells (density of 1.0 × 10^4 cells per piece) were cultured in polyvinyl-alcohol-based scaffolds for 24 h and then incubated with the different mechanical strength hydrogel at a cyclic compression pressure (20 and 40 kPa were applied at 0.5 Hz) up to 24 h. After 24 h of incubation, a 20 μL/well MTT solution (PBS solvent) was added into each well. After 4 h of culturing, the culture medium was thrown away and replaced with a 150 μL/well DMSO solvent. The DMSO solvent was measured at 570 nm using a microplate reader. After culturing for 24 h, the FLS were stained with Annexin V and propidium iodide (PI) following the operating instructions for flow cytometry analysis.

4.6. RT-qPCR Analysis. Total mRNA was extracted by the Trizol reagent after culturing for 14 days. cDNA was

synthesized using the PrimeScript RT reagent kit. Amplification reactions were set up in 96-well plates using the iTaq SYBR Green Supermix. These analyses were conducted to detect IL6, IL1β, MMP-1, and TNF-α expressions, in which β-actin was used as an internal control group. The primer sequences are listed in Table 1.

4.7. Western Blot Analysis. The FLS were collected and boiled in sample-loading buffer for 10 min at 95 °C. The proteins were electrophoretically resolved on a 12% SDS-PAGE gel at 120 V and transferred to PVDF membranes. The PVDF membrane was then blotted with primary antibodies at 4 °C overnight. The PVDF membrane was washed with TBST and then incubated with peroxidase-conjugated secondary antibodies. The chemiluminescent signal was visualized according to the manufacturer's instruction. Primary antibodies targeting the following proteins were used: p-IKBα (phosphor S36, ab133462, Abcam), IKBα (ab76429, Abcam), p-p65 (phospho S276, ab183559, Abcam), p65 (ab16502, Abcam), IL-6 (ab233706, Abcam), MMP-1 (ab134184, Abcam), and β-actin (ab115777, Abcam).

4.8. Animal Operation. Fifty Sprague Dawley rats (210 ± 10 g, 7 weeks and specific pathogen-free) were obtained from Guangdong Medical Laboratory Animal Center (Guangzhou, China). To simulate the interference of the AI drug, only female rats were used. All rats were housed in a controlled environment (22 ± 2 °C; 70% humidity; nature-simulated light/dark cycle) and had free access to a planned diet with the AI drug. All rats were fed for 5 weeks with the AI drug before the experiments. Then, the rats were intra-articularly injected with ~35 μL of three kinds of mechanical strength hydrogels for 2 weeks. All experiments were performed in accordance with the standard of the Animal Ethics Committee of Jinan University Laboratory Animal Ethics, Guangzhou, China (20190611216528).

4.9. Intra-articular Sample Preparation. After ~35 μL of hydrogels was injected for 2 weeks, the intra-articular fluid was obtained from the synovial cavity of both knees, and ~35 μL of PBS was recovered. The intra-articular fluid was reserved for ELISA analysis. All rats in the AI model were sacrificed at the second week under anesthesia, and the left knee joint was harvested by cutting the femur and tibia/fibula. After removing the muscles from the joint, the latter was fixed in 4% paraformaldehyde solution at room temperature for 7 days. The synovial tissue was cut by ophthalmic scissors and collected carefully for immunohistochemical analysis. All tissues were stored at −80 °C until further experiments.

4.10. ELISA of IL6 and MMP-1. IL6 and MMP-1 levels in the intra-articular lavage fluid (IALF) of the knee were determined using IL6 and MMP-1 ELISA kits (Bio-Rad Laboratories, CA, USA) according to the manufacturer's instructions. All the total proteins were measured to equalize the ratio of dilution. For each marker, the data were normalized by dividing the pg/mL values for the corresponding tissue.

4.11. Identification of Synovial Tissues by Immunohistochemistry (IHC). The rat synovial tissue was collected following *in vivo* injection of hydrogels and detected using mouse monoclonal antibody against IL-6 (ab6672, Abcam) and MMP-1 (ab52631, Abcam) for 2 weeks. Tissue sections were then deparaffinized, rehydrated, incubated in citrate buffer, and blocked with 3% H_2O_2. The sections were then blocked with 1% BSA and stained with primary antibodies (1:50) overnight. The sections were then incubated with the

secondary antibody against mouse IgG (1:500) for 30 min at 37 °C. Then, the sections were incubated by the streptavidin-HRP and diaminobenzidine (DAB) substrate. The control group was obtained following the same procedures but without any hydrogel injection, and the other contrast groups were low-intensity, moderate-intensity, and high-intensity hydrogels group, respectively.

4.12. Statistical Analysis. Data were evaluated using GraphPad Prism 6 software followed by the Student's unpaired t test. We define $p < 0.05$ as statistically significant. The statistical data were presented as the means ± SD.

■ AUTHOR INFORMATION

Corresponding Authors

Wenqiang Li − *Guangzhou Sport University, Guangzhou 510500, China;* ⓞ orcid.org/0000-0002-1498-2258; Email: 405119923@qq.com

Liping Wang − *UniSA Cancer Research Institute, UniSA Clinical & Health Sciences, University of South Australia, Adelaide, SA 5001, Australia;* ⓞ orcid.org/0000-0001-9355-1167; Email: liping.wang@mymail.unisa.edu.au

Zi-Guo Yuan − *Laboratory of Parasitology College of Veterinary Medicine, South China Agricultural University, Guangzhou 510000, China;* Email: ziguoyuan@scau.edu.cn

Authors

Zipeng Yang − *Laboratory of Parasitology College of Veterinary Medicine, South China Agricultural University, Guangzhou 510000, China*

Chang-Peng Xu − *Department of Orthopaedics, Guangdong Second Provincial General Hospital, Guangzhou, Guangdong 510317, P.R. China*

Yuhui Chen − *Orthopedic Hospital of Guangdong Province, Department of Orthopedic Surgery, The Third Affiliated Hospital of Southern Medical University, Guangzhou 510630, China*

Complete contact information is available at:
https://pubs.acs.org/10.1021/acsomega.1c00580

Notes

The authors declare no competing financial interest.

■ REFERENCES

(1) Irwin, M. L.; Cartmel, B.; Gross, C. P.; Ercolano, E.; Li, F.; Yao, X.; Fiellin, M.; Capozza, S.; Rothbard, M.; Zhou, Y.; et al. Randomized exercise trial of aromatase inhibitor-induced arthralgia in breast cancer survivors. *J. Clin. Oncol.* **2015**, *33*, 1104−1111.

(2) Wright, L. E.; Harhash, A. A.; Kozlow, W. M.; Waning, D. L.; Regan, J. N.; She, Y.; John, S. K.; Murthy, S.; Niewolna, M.; Marks, A. R.; Mohammad, K. S.; Guise, T. A. Aromatase inhibitor-induced bone loss increases the progression of estrogen receptor-negative breast cancer in bone and exacerbates muscle weakness in vivo. *Oncotarget* **2017**, *8*, 8406−8419.

(3) Niravath, P. Aromatase inhibitor-induced arthralgia: a review. *Ann. Oncol.* **2013**, *24*, 1443−1449.

(4) van Hellemond, I. E. G.; Geurts, S. M. E.; Tjan-Heijnen, V. C. G. Current Status of Extended Adjuvant Endocrine Therapy in Early Stage Breast Cancer. *Curr. Treat. Options Oncol.* **2018**, *19*, 26.

(5) Chim, K.; Xie, S. X.; Stricker, C. T.; Li, Q. S.; Gross, R.; Farrar, J. T.; DeMichele, A.; Mao, J. J. Joint pain severity predicts premature discontinuation of aromatase inhibitors in breast cancer survivors. *BMC Cancer* **2013**, *13*, 401.

(6) Bauml, J.; Chen, L.; Chen, J.; Boyer, J.; Kalos, M.; Li, S. Q.; DeMichele, A.; Mao, J. J. Arthralgia among women taking aromatase inhibitors: is there a shared inflammatory mechanism with co-morbid fatigue and insomnia? *Breast Cancer Res.* **2015**, *17*, 89.

(7) Maia, H., Jr.; Haddad, C.; Coelho, G.; Casoy, J. Role of inflammation and aromatase expression in the eutopic endometrium and its relationship with the development of endometriosis. *Womens Health* **2012**, *8*, 647−658.

(8) Pluchino, N.; Poppi, G.; Yart, L.; Marci, R.; Wenger, J. M.; Tille, J. C.; Cohen, M. Effect of local aromatase inhibition in endometriosis using a new chick embryo chorioallantoic membrane model. *J. Cell Mol. Med.* **2019**, *23*, 5808−5812.

(9) Wright, C. L.; Hoffman, J. H.; McCarthy, M. M. Evidence that inflammation promotes estradiol synthesis in human cerebellum during early childhood. *Transl. Psychiatry* **2019**, *9*, 58.

(10) Capellino, S.; Straub, R. H.; Cutolo, M. Aromatase and regulation of the estrogen-to-androgen ratio in synovial tissue inflammation: common pathway in both sexes. *Ann. N. Y. Acad. Sci.* **2014**, *1317*, 24−31.

(11) Zhang, J.-M.; An, J. Cytokines, inflammation and pain. *Int. Anesthesiol. Clin.* **2007**, *45*, 27.

(12) Assis, L.; Milares, L. P.; Almeida, T.; Tim, C.; Magri, A.; Fernandes, K. R.; Medalha, C.; Muniz Renno, A. C. Aerobic exercise training and low-level laser therapy modulate inflammatory response and degenerative process in an experimental model of knee osteoarthritis in rats. *Osteoarthritis Cartilage* **2016**, *24*, 169−177.

(13) Hurley, M.; Dickson, K.; Hallett, R.; Grant, R.; Hauari, H.; Walsh, N.; Stansfield, C.; Oliver, S.; Cochrane Musculoskeletal Group. Exercise interventions and patient beliefs for people with hip, knee or hip and knee osteoarthritis: a mixed methods review. *Cochrane Database Syst. Rev.* **2018**, *4*, No. Cd010842.

(14) Bustamante, M. F.; Garcia-Carbonell, R.; Whisenant, K. D.; Guma, M. Fibroblast-like synoviocyte metabolism in the pathogenesis of rheumatoid arthritis. *Arthritis Res. Ther.* **2017**, *19*, 110.

(15) Jamal, J.; Roebuck, M. M.; Lee, S. Y.; Frostick, S. P.; Abbas, A. A.; Merican, A. M.; Teo, S. H.; Wood, A.; Tan, S. L.; Bou-Gharios, G.; et al. Modulation of the mechanical responses of synovial fibroblasts by osteoarthritis-associated inflammatory stressors. *Int. J. Biochem. Cell Biol.* **2020**, *126*, 105800.

(16) Malemud, C. J. Matrix Metalloproteinases and Synovial Joint Pathology. *Prog. Mol. Biol. Transl. Sci.* **2017**, *148*, 305−325.

(17) Nazet, U.; Grässel, S.; Jantsch, J.; Proff, P.; Schröder, A.; Kirschneck, C. Early OA Stage Like Response Occurs after Dynamic Stretching of Human Synovial Fibroblasts. *Int. J. Mol. Sci.* **2020**, *21*, 3874.

(18) Bader, R. A.; Wagoner, K. L. Modulation of the response of rheumatoid arthritis synovial fibroblasts to proinflammatory stimulants with cyclic tensile strain. *Cytokine+* **2010**, *51*, 35−41.

(19) Yang, G.; Im, H.-J.; Wang, J. H.-C. Repetitive mechanical stretching modulates IL-1β induced COX-2, MMP-1 expression, and PGE2 production in human patellar tendon fibroblasts. *Gene* **2005**, *363*, 166−172.

(20) Tilleman, K.; Van Steendam, K.; Cantaert, T.; De Keyser, F.; Elewaut, D.; Deforce, D. Synovial detection and autoantibody reactivity of processed citrullinated isoforms of vimentin in inflammatory arthritides. *Rheumatology* **2008**, *47*, 597−604.

(21) Miller, R. E.; Miller, R. J.; Malfait, A. M. Osteoarthritis joint pain: the cytokine connection. *Cytokine+* **2014**, *70*, 185−193.

(22) Muller-Ladner, U.; Neumann, E.; Meier, F. M. P.; Lefevre, S. J. C. P. D. Role of Synovial Fibroblasts in Rheumatoid Arthritis. 2015, *21* (2), 1.

(23) Yamaura, M.; Yao, M.; Yaroslavsky, I.; Cohen, R.; Smotrich, M.; Kochevar, I. E. Low level light effects on inflammatory cytokine production by rheumatoid arthritis synoviocytes. *Lasers Surg. Med.* **2009**, *41*, 282−290.

(24) Zhang, Y.; Huang, W.; Jiang, J.; Xie, J.; Xu, C.; Wang, C.; Yin, L.; Yang, L.; Zhou, K.; Chen, P.; et al. Influence of TNF-α and biomechanical stress on matrix metalloproteinases and lysyl oxidases expressions in human knee synovial fibroblasts. *Knee Surg. Sports Traumatol. Arthrosc.* **2014**, *22*, 1997−2006.

(25) Makarov, S. S. NF-kappa B in rheumatoid arthritis: a pivotal regulator of inflammation, hyperplasia, and tissue destruction. *Arthritis Res.* **2001**, *3*, 200−206.

(26) Gomez, P. F.; Pillinger, M. H.; Attur, M.; Marjanovic, N.; Dave, M.; Park, J.; Bingham, C. O., III; Al-Mussawir, H.; Abramson, S. B. Resolution of inflammation: prostaglandin E2 dissociates nuclear trafficking of individual NF-kappaB subunits (p65, p50) in stimulated rheumatoid synovial fibroblasts. *J. Immunol.* **2005**, *175*, 6924−6930.

(27) Morisugi, T.; Tanaka, Y.; Kawakami, T.; Kirita, T. Mechanical stretch enhances NF- B-dependent gene expression and poly(ADP-ribose) synthesis in synovial cells. *J. Biochem.* **2010**, *147*, 633−644.

(28) Wang, H.; Williams, G. R.; Wu, J.; Wu, J.; Niu, S.; Xie, X.; Li, S.; Zhu, L.-M. Pluronic F127-based micelles for tumor-targeted bufalin delivery. *Int. J. Pharm.* **2019**, *559*, 289−298.